Breakup of ^{6}Li + p at near-barrier energies and the effect on elastic scattering

V. Soukeras,[1] A. Pakou,[1,*] F. Cappuzzello,[2,3] L. Acosta,[4,5] C. Agodi,[2] N. Alamanos,[6] S. Calabrese,[2,3] D. Carbone,[2] M. Cavallaro,[2] A. Cunsolo,[2] A. Di Pietro,[2] J. P. Fernández-García,[2] P. Figuera,[2] M. Fisichella,[2] A. Foti,[3,5] N. Keeley,[7] G. Marquìnez-Duràn,[8] I. Martel,[8] M. Mazzocco,[9,10] D. Pierroutsakou,[11] K. Rusek,[12] G. Santagati,[2,3] O. Sgouros,[1] E. Stiliaris,[13] E. Strano,[9,10] D. Torresi,[9,10] and K. Zerva[1]

[1]*Department of Physics and HINP, University of Ioannina, 45110 Ioannina, Greece*
[2]*INFN Laboratori Nazionali del Sud, via S. Sofia 62, 95125, Catania, Italy*
[3]*Dipartimento di Fisica e Astronomia, Universita di Catania, via S. Sofia 64, 95125, Catania, Italy*
[4]*Instituto de Fisica, Universidad Nacional Autonoma de Mexico, Mexico D. F. 01000, Mexico*
[5]*INFN–Sezione di Catania, via S. Sofia 64, 95125, Catania, Italy*
[6]*CEA-Saclay, DAPNIA-SPhN, 91191, Gif-sur-Yvette, France*
[7]*National Centre for Nuclear Research, Andrzeja Sołtana 7, 05-400, Otwock, Poland*
[8]*Departamento di Fisica Aplicada, Universidad de Huelva, E-21071, Huelva, Spain*
[9]*Departimento di Fisica e Astronomia, Universita di Padova, via Marzolo 8, I-35131, Padova, Italy*
[10]*INFN–Sezione di Padova, via Marzolo 8, I-35131, Padova, Italy*
[11]*INFN–Sezione di Napoli, via Cinthia, I-80126, Napoli, Italy*
[12]*Heavy Ion Laboratory, University of Warsaw, Pasteura 5a, 02-093, Warsaw, Poland*
[13]*Institute of Accelerating Systems and Applications and Department of Physics, University of Athens, Greece*

(Received 2 March 2017; published 18 May 2017)

Exclusive breakup measurements have been performed for the ^{6}Li + p system in inverse kinematics at ^{6}Li incident energies of 25 and 29 MeV. The results are considered in the Continuum Discretized Coupled-Channels framework, together with elastic scattering data at 16, 20, 25, and 29 MeV, obtained simultaneously in the same experiment and reported previously. Good agreement between data and theory is observed, interpreted as evidence for strong coupling to the continuum. The direct and sequential (via the ^{6}Li 3_1^+ resonance) breakup cross sections are found to be equally large at the higher incident energies but the dominant effect on the elastic scattering is due to coupling to the sequential breakup. This effect remains dominant even at the lowest energy of 16 MeV, despite the negligible cross section for excitation of the resonance at this low incident energy.

DOI: 10.1103/PhysRevC.95.054614

I. INTRODUCTION

Many weakly bound nuclei possess a single bound state, the ground state, and a broad featureless continuum plus a small number of low-lying unbound resonant states. Due to their low binding energies, they may be easily excited above their particle emission thresholds; hence the breakup of such nuclei induced by the Coulomb and nuclear fields of suitable targets could be a useful tool to investigate their structure and benchmark coupling effects on their elastic scattering. The simplest breakup process occurs for interaction with a proton target, with excitation mainly by the nuclear field. In addition, nucleon scattering is one of the simplest and most valuable tools for probing the structure of a nucleus. For measurements of this type involving radioactive nuclei, the inverse kinematics technique is adopted whereby a beam of the radioactive species of interest is incident on a proton-rich target, and the halo or skin-like nature of the projectile may be probed as long as the potential is known. It was shown previously [1,2] that at energies 3 to 6 times the Coulomb barrier the microscopic potential of Jeukenne, Lejeune, and Mahaux (JLM) [3] without any couplings to continuum is not adequate to describe the elastic scattering data for ^{6,7}Li on protons, with these light nuclei being strictly speaking outside its range of validity. On the other hand, the Continuum Discretized Coupled-Channels (CDCC) approach, where couplings to the continuum are explicitly taken into account, describes these data very well. However, for a more effective interpretation of experimental data in a coupled channel scheme, a global description of all the reaction channels involved is required. In this spirit, we present here systematic breakup measurements in their own right and also as complementary measurements to existing elastic scattering and ^{6}Li + $p \rightarrow$ ^{4}He + ^{3}He data. These latter two measurements were made under the same experimental conditions as the present data and have been previously analyzed [1,4] but will be reconsidered in this study as part of a global picture.

The ^{6}Li nucleus exhibits a pronounced cluster structure with a very low binding energy in the α-d channel of 1.47 MeV. Therefore, breakup is expected to be significant in reactions involving this nucleus. It has mainly been investigated in exclusive measurements at near-barrier energies on light [5,6], medium [7–11], and heavy targets [12–20]. Interest has also been shown in the effect of breakup on the elastic scattering [21–23]. The only existing breakup measurement, p + ^{6}Li, reported in Ref. [24], was performed at energies well above the Coulomb barrier ($\sim 12 \times V_C$). Moreover, neither the total breakup cross section nor angular distributions in the center-of-mass system are given in

*Corresponding author: apakou@cc.uoi.gr

Ref. [24] so comparisons with the present work cannot be made.

In the following sections, we will first present the details of the experimental setup and the data reduction procedure (Sec. II), then we will proceed with details of our theoretical calculations (Sec. III), discussing the effect of breakup coupling on the elastic scattering, and finally we will present our concluding remarks (Sec. IV).

II. EXPERIMENTAL DETAILS AND DATA REDUCTION

The experiment was performed at the MAGNEX facility of the Istituto Nazionale di Fisica Nucleare Laboratori Nazionali del Sud (INFN-LNS) in Catania, Italy. Beams of $^6Li^{3+}$ ions were accelerated by the TANDEM accelerator for elastic scattering measurements at energies of 16, 20, 25, and 29 MeV and impinged on a $240\,\mu g/cm^2$ CH_2 target. Experimental details and an analysis of the elastic scattering data were reported previously in Ref. [1]. A breakup measurement was performed at the two higher energies, 25 and 29 MeV (4.17 MeV/u and 4.83 MeV/u), employing a thicker target of 308 $\mu g/cm^2$ to improve statistics. The α fragments were momentum analyzed by the MAGNEX spectrometer [25–27], whose optical axis was set at $\theta_{opt} = 4^\circ$, subtending an angular range between -1 to 10°, and were detected by its focal plane detectors [28,29]. MAGNEX worked with full horizontal angular acceptance and a rather well-open vertical acceptance as the counting rate due to breakup was rather low. The elastically scattered ^{6}Li ions were swept out by the chosen magnetic fields, which allowed the detection of α particles in energy slices of 8.4 to 13.3 MeV and 11 to 15.5 MeV for the 25- and 29-MeV runs, respectively. A small remnant of elastic scattering was rejected off-line by the appropriate cuts in two-dimensional $E - (\Delta E + E)$ spectra, obtained via the gas (ΔE denotes the energy loss in the gas) and silicon (E denotes the residual energy in the silicon detectors) detectors of the focal plane [28,29]. Our data reduction technique, based on the ray reconstruction of the data, is described in Refs. [30–33].

The second breakup fragments (the deuterons) were detected in a silicon detector fixed at $\theta_{lab} = 5^\circ$, subtending an angular range between $4.2^\circ \leqslant \theta_{lab} \leqslant 5.8^\circ$. To prevent deterioration from Rutherford scattering, this detector was masked by 30.8- and 43.6-μm tantalum foils for the measurements at 25 and 29 MeV, respectively. These foils absorbed all heavy particles but allowed protons and deuterons associated with the energy of the first solution to the double-valued equation of the reaction kinematics to pass through. Light particles associated with energies of the second kinematic solution were blocked by these foils, and therefore our data are limited to the forward angular range (10° to 90°) in the center-of-mass frame. This was, however, a minor problem for the extraction of the total breakup yield since the angular distribution of the breakup fragments is predicted to be flat by our calculations.

Exclusive yields were determined for pairs of angles every 0.5° for α particles observed in MAGNEX over the angular range 0° to 10°, combined with deuterons observed in the fixed angle detector at 5°. Two-dimensional spectra for the 25- and 29-MeV runs displaying the energy of α particles recorded in MAGNEX versus the energy of deuterons or recoiling protons detected in the 5° detector are shown in Figs. 1 and 2. One-dimensional coincidence spectra from the 5° detector are shown in Figs. 3 and 4 for the 25- and 29-MeV runs, respectively. It is evident that the recoiling protons are well discriminated from the deuterons. In the two-dimensional spectra, the loci at the extreme right are due to carbon, present in the CH_2 target. It should be noted that the background due to carbon was of the order of ~11% to 15% and hardly affected the main breakup data. This can be more clearly seen in the one-dimensional coincidence spectra displayed in Figs. 3 and 4. Superimposed on these spectra are spectra obtained with a carbon target (shown in green), appropriately normalized, reflecting this background.

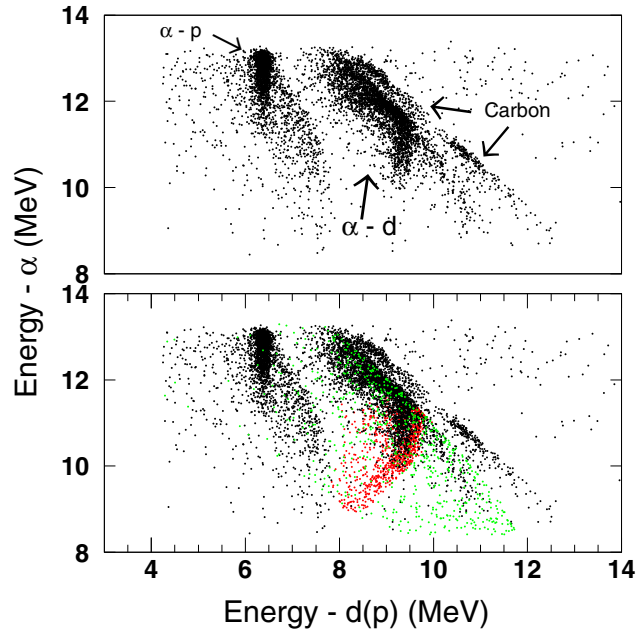

FIG. 1. Upper figure: Two-dimensional plot at 25 MeV (4.17 MeV/u) representing coincident events of the two ^{6}Li breakup fragments. Energy of α particles (energy α) vs energy of deuterons or recoiling protons (energy $d(p)$). The α particles were detected in the MAGNEX spectrometer over the angular range $\theta_{lab} = 0$ to 10°, while the deuterons and the recoiling protons were detected in a silicon detector fixed at $\theta_{lab} = 5^\circ$. The observed loci for α-p coincidences and α-d coincidences due to breakup of ^{6}Li on protons and α-d coincidences due to breakup on carbon are indicated on the figure. Lower figure: Superimposed on the experimental spectrum, denoted by the black dots, are simulated events for the first kinematic solution of the resonant and direct breakup, denoted by the red and green dots, respectively.

The exclusive yields were transferred to laboratory double differential cross sections ($d^2\sigma/d\Omega_\alpha d\Omega_d$) using a detection efficiency estimated through a Monte Carlo three-body simulation code [34,35]. Our code takes into account the $^6Li + p$ reaction, leading to an excited state of $^6Li^*$ with an angular distribution determined in the CDCC calculation to be described below. The ^{6}Li acquires randomly an energy inside one of the energy bins as specified in the CDCC framework. This includes either the resonant bin at 2.186 MeV (0.716 MeV above the breakup threshold), or any one of the continuum bins.

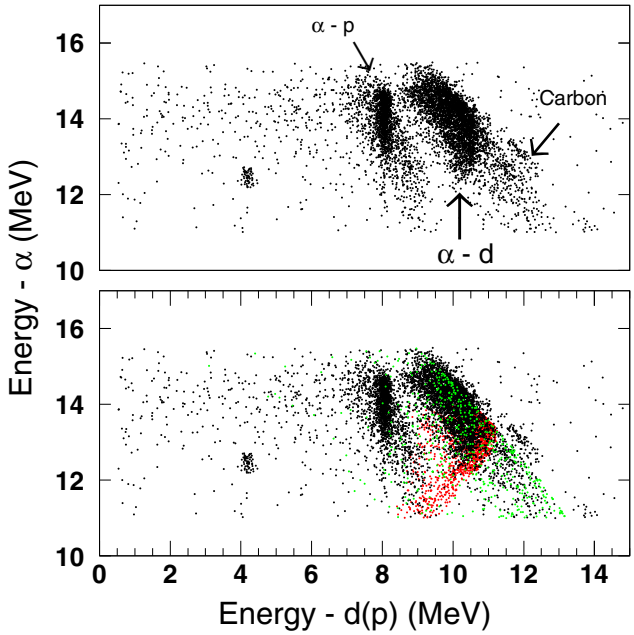

FIG. 2. Same as in Fig. 1 but for 29 MeV (4.83 MeV/u).

The excited lithium breaks into two fragments, α and deuteron, with one emitted with a randomly assigned specific energy and momentum and the second with energy and momentum fulfilling the conservation laws in the rest frame of ^{6}Li*. The energy distributions of the fragments thus obtained in the rest frame of ^{6}Li* are transformed to the laboratory system by imposing a Galilean transformation followed by the appropriate rotation. The results of our simulation for the energy distributions are presented in the two-dimensional α versus deuteron energy spectra in Figs. 1 and 2 and the one-dimensional spectra for deuterons in Figs. 3 and 4 for the 25- and 29-MeV runs, respectively. In the two-dimensional spectra, the red dots denote the simulation of sequential breakup via the 3_1^+ resonance while the green dots denote the simulation of direct, nonresonant breakup. The very good agreement between the experimental data and the simulation based on the CDCC binning of the continuum confirms the realistic philosophy behind this theoretical approach. It should be noted that another process which could contribute to α-d coincidences is the neutron-stripping reaction: $^6\mathrm{Li} + p \rightarrow {}^5\mathrm{Li} + d \rightarrow \alpha + p + d$, with a Q value of -3.44 MeV, which, however, according to preliminary calculations, is expected to have very low probability. The results of a simulation of this process shown on Figs. 3 and 4 by dashed blue lines show clearly that it does not affect the breakup data.

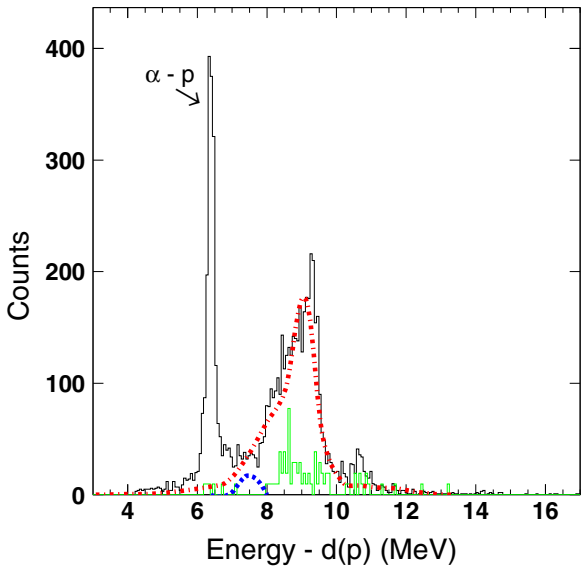

FIG. 3. Exclusive breakup spectrum, acquired in the 5° silicon detector with a CH_2 target at 25 MeV (α-d or p coincidences). The results of simulations of the first kinematic solution for α-d coincidences are denoted by the dot-dashed red line. The peak at the left corresponds to α coincidences with the recoiling protons. The spectrum in green represents an exclusive spectrum acquired with a carbon target, appropriately normalized. The dashed blue line represents a simulation of the $^6\mathrm{Li} + p \rightarrow {}^5\mathrm{Li} + d \rightarrow \alpha + p + d$ reaction, arbitrarily normalized (see text).

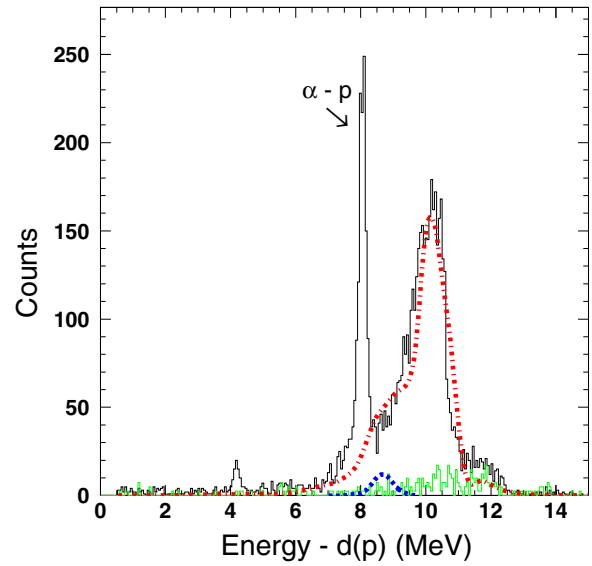

FIG. 4. Same as in Fig. 3 but for 29 MeV (4.83 MeV/u).

III. THEORETICAL DETAILS: CDCC CALCULATIONS

For the CDCC calculations, we follow the same technique as in Ref. [36], where we present calculations for the same system but at a much higher energy, 155 MeV (25.8 MeV/A).

An $\alpha + d$ cluster model of ^{6}Li was adopted, with all the parameters of the model including discretization and truncation described in detail in Refs. [1,37]. In addition to the nonresonant continuum, the 3_1^+ resonance was taken into account and was treated as a momentum bin with a width corresponding to 0.1 MeV. The central parts of the $^6\mathrm{Li} + p$ optical potentials were derived as previously [36] from empirical $p + \alpha$ and $p + d$ potentials using the Watanabe single-folding method. The optical potentials were obtained from existing $p + d$ and $p + \alpha$ elastic scattering

TABLE I. Optical model potentials for the $^4\mathrm{He}+p$ system deduced by fitting existing data [43,44] adopting a Woods-Saxon potential (real and imaginary volume terms). The nuclear radius was $R_{V(W)} = r_{V(W)} \times 4^{1/3}$ fm and the Coulomb radius was $R_C = 1.25 \times 4^{1/3}$ fm.

E (MeV)	V (MeV)	r_V (fm)	a_V (fm)	W (MeV)	r_W (fm)	a_W (fm)
29	49.811	1.10	0.477	0.040	1.10	0.477
25	52.278			0.039		
20	55.567			0.038		
16	58.230			0.037		

studies at $E = 2.52$ to 5 MeV/u [38–44]. These $p+d$ and $p+\alpha$ elastic scattering data were fitted by simple Woods-Saxon form factors with real volume and imaginary volume parts for the $p+\alpha$ system and real volume and surface imaginary terms for the $p+d$ system. The optical model potential parameters are given in Tables I and II for the $p+\alpha$ and $p+d$ systems, respectively. A proton spin-orbit potential of Thomas form with parameters $V_{so} = 4.26$ MeV, $r_{so} = 1.10$ fm, and $a_{so} = 0.35$ fm was added to the diagonal $^6\mathrm{Li}+p$ Watanabe folding potentials. These potentials were fed into FRESCO calculations [45]. The output of this code gives angular distributions for both elastic scattering and breakup.

The breakup results are compared with the data in Figs. 5 and 6 for the 25- and 29-MeV runs, respectively. They are in satisfactory agreement, although the general trend is for the calculations to underestimate the data. The experimental breakup cross sections, obtained by integration of the experimental angular distributions extended to all angles assuming the CDCC calculation shape, are given in Table III. The calculated elastic scattering angular distributions are compared with the data obtained in the same experiment and reported previously [1] in Figs. 7, 8, 9, and 10. For the sake of completeness, we present here the elastic scattering data at all four energies, i.e., 16, 20, 25, and 29 MeV. Since we wished to investigate the effect of coupling to breakup on the elastic scattering, we also performed one-channel (no coupling) calculations and calculations with coupling to direct excitation of the continuum only, omitting coupling to the 3_1^+ resonance. All theoretical results, full CDCC, one-channel, and CDCC with coupling to direct breakup only are compared with the data in Figs. 7, 8, 9, and 10 for 16, 20, 25, and

TABLE II. Optical model potentials for the $^2\mathrm{H}+p$ system deduced by fitting existing data [38–42] adopting a Woods-Saxon potential (real volume and imaginary surface terms). The nuclear radius was $R_{V(W)} = r_{V(W)} \times 1^{1/3}$ fm and the Coulomb radius was $R_C = 1.30 \times 1^{1/3}$ fm.

E (MeV)	V (MeV)	r_V (fm)	a_V (fm)	W (MeV)	r_W (fm)	a_W (fm)
29	66.958	1.25	0.501	0.715	1.20	0.517
25	70.274			0.700		
20	74.696			0.679		
16	78.276			0.663		

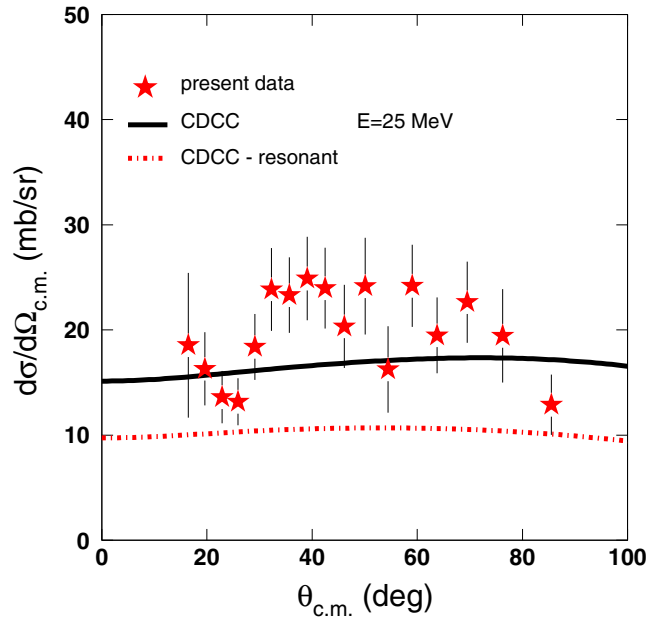

FIG. 5. Experimental and theoretical angular distributions in the center of mass for the breakup of ^{6}Li on a proton target at 25 MeV (4.17 MeV/u). The experimental data, referring to the first kinematic solution, are shown by the filled red stars. The solid black line represents the full CDCC calculation. The dot-dashed red line denotes the result of a CDCC calculation taking into account coupling to the 3_1^+ resonant state only.

29 MeV, respectively. As can be seen, in general coupling to the continuum is strong and the full CDCC calculations describe the elastic scattering reasonably well at all energies. Moreover, we find that coupling to direct breakup makes a very slight change from the one-channel calculation and therefore the important coupling is that to the resonant breakup.

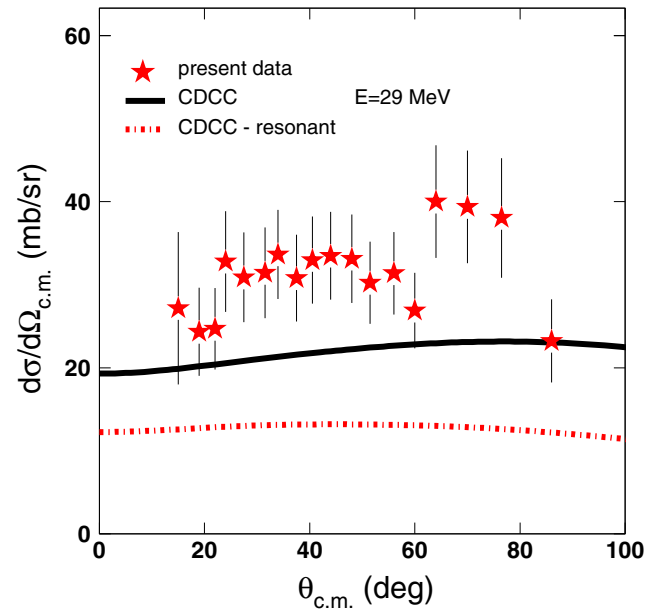

FIG. 6. Same as in Fig. 5 but for 29 MeV (4.83 MeV/u).

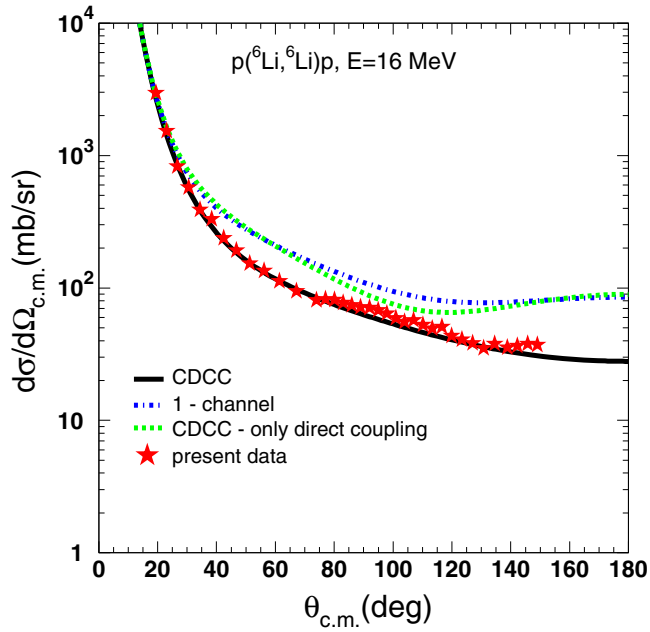

FIG. 7. Elastic scattering of ^{6}Li + p at 16 MeV (2.67 MeV/u). The data are compared with full CDCC calculations (solid black line), one-channel calculations (dot-dashed blue line), and calculations with coupling to direct breakup only (dashed green line). The uncertainty of the experimental data is included in the size of the stars.

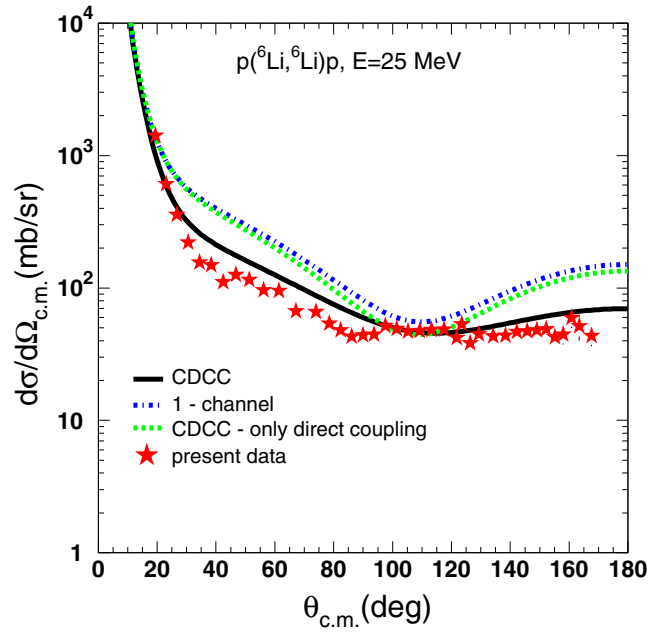

FIG. 9. Same as in Fig. 7 but for 25 MeV (4.17 MeV/u).

IV. DISCUSSION AND SUMMARY

We have measured the exclusive breakup of ^{6}Li on a proton target at two near-barrier energies, 25 and 29 MeV (4.17 and 4.83 MeV/u) in inverse kinematics. The α fragments were measured in the MAGNEX spectrometer spanning an angular range from 0 to 10°, in coincidence with the deuteron fragments detected in a silicon detector fixed at 5°. Due to the specific experimental conditions, that is, the mask in front of the 5° detector, events with energies corresponding to the second kinematic solution were not observed and the angular range of the measurement was limited to forward angles. In a global interpretation of the data within the CDCC approach, our study included comparisons between theory and simultaneous measurements of elastic scattering and breakup angular distributions as well as total breakup and absorption cross sections, the last two included in Table III.

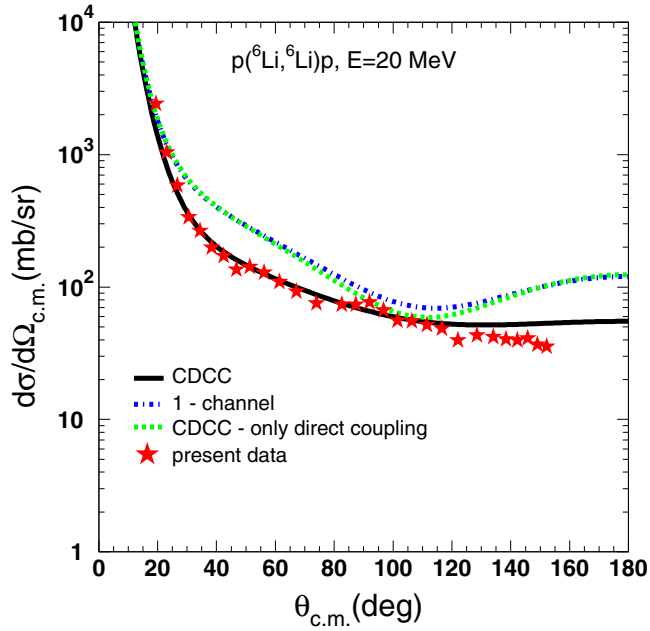

FIG. 8. Same as in Fig. 7 but for 20 MeV (3.33 MeV/u).

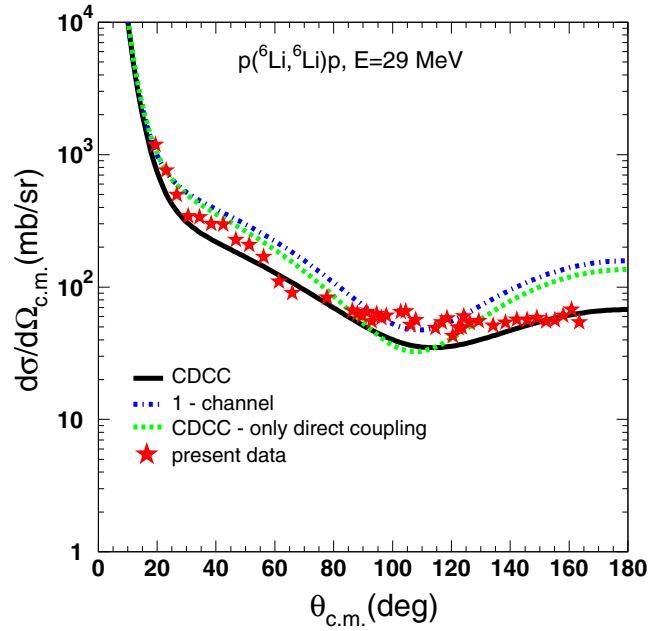

FIG. 10. Same as in Fig. 7 but for 29 MeV (4.83 MeV/u).

TABLE III. Reaction cross sections for the ^{6}Li + p system: Experimental breakup cross sections, σ_{br}, CDCC breakup cross sections (in parentheses the sequential breakup cross section via the 3_1^+ resonance), σ_{br}^C, absorption cross sections according to CDCC, σ_{abs}^C, experimental absorption cross sections measured previously via the ^{6}Li + $p \rightarrow {}^4$He + ^{3}He reaction, σ_{abs} [4].

E (MeV)	σ_{br} (mb)	σ_{br}^C (mb)	σ_{abs}^C (mb)	σ_{abs} (mb)
29	370 ± 64	269.4(143.3)	109.5	95 ± 2
25	235 ± 46	200.0(117.0)	133.0	131 ± 6
20		102.9(37.5)	162.0	140 ± 8
16		69.7(0.03)	130.7	111 ± 2

Overall, the interpretation of the data in this framework was found to be satisfactory. In more detail, the agreement of the theoretical with the experimental elastic scattering angular distributions was good, while the description of the breakup angular distributions was reasonable but with some tendency of theory to underpredict the data. The effect of breakup coupling on the elastic channel was strong, with the most significant contribution coming from sequential breakup via the first resonance at 2.186 MeV. This is in accordance with similar findings for medium and heavy mass targets [22,23].

From an inspection of Table III, where in the third column we present total breakup cross sections and in parentheses sequential breakup cross sections via the 3_1^+ resonance, we can conclude that the sequential breakup accounts for ∼50% of the total breakup for the highest two energies, ∼38% at 20 MeV and almost zero for the lowest energy, 16 MeV. However, the importance of the influence of breakup coupling on the elastic scattering is not correlated with the magnitude of the breakup cross section; for example, at the lowest energy of 16 MeV coupling to the sequential breakup via the 3_1^+ resonance had the strongest influence, while the cross section for this breakup mode was almost zero (see Table III), thus presenting an example of a "virtual" coupling effect. A similar situation was met with for the elastic scattering of ^{7}Li from a proton target recently reported in Ref. [35]. In that case, the cross section for excitation of the first $(7/2^-)$ $\alpha + t$ resonance was determined to be ∼0.5 mb compared a total breakup of 66 mb, while the coupling to resonant breakup was found to be dominant. It is also important to make comparisons with other observables deduced from the CDCC calculations, for example, the absorption. In Table III, the calculated absorption cross sections are compared with experimental values for the ^{6}Li + $p \rightarrow {}^4$He + ^{3}He reaction, the only other available reaction channel at these energies, measured simultaneously with the breakup but reported in Ref. [4]. The agreement with the data is very good, giving further support to a global interpretation of the ^{6}Li + p reaction in the CDCC framework and the validity of the experimental data.

In summary, the present exclusive breakup measurements for the ^{6}Li + $p \rightarrow \alpha + d + p$ process, performed for the first time at near-barrier energies ($\sim 5 \times V_C$), considered together with elastic scattering data and cross sections for the ^{6}Li + $p \rightarrow {}^4$He + ^{3}He reaction channel, present in total good agreement with CDCC calculations. The cross sections for sequential breakup via the 3_1^+ resonance at 2.186 MeV are strong for ^{6}Li incident energies of 29, 25, and 20 MeV and coupling to this breakup mode has the most important effect on the elastic scattering. By contrast, while direct breakup to the nonresonant continuum is also substantial—with cross sections comparable to or greater than those for sequential breakup at ^{6}Li incident energies of 29, 25, and 20 MeV—its coupling effect on the elastic scattering is unimportant. At the lowest ^{6}Li incident energy of 16 MeV, we find an example of a "virtual" coupling effect, where although the sequential breakup cross section is almost zero it remains the dominant coupling influence on the elastic scattering.

ACKNOWLEDGMENTS

We warmly acknowledge the TANDEM operators of LNS for the production and delivery of the ^{6}Li beams. The research leading to these results was partially funded by the European Union Seventh Framework Programme FP7/2007-2013 under Grant Agreement No. 262010-ENSAR.

[1] V. Soukeras, A. Pakou, F. Cappuzzello *et al.*, Phys. Rev. C **91**, 057601 (2015).
[2] A. Pakou, V. Soukeras, and F. Cappuzzello, Phys. Rev. C **94**, 014604 (2016).
[3] J.-P. Jeukenne, A. Lejeune, and C. Mahaux, Phys. Rev. C **16**, 80 (1977).
[4] Ch. Betsou, A. Pakou, F. Cappuzzello *et al.*, Eur. Phys. J. A **51**, 86 (2015).
[5] A. Pakou, N. Alamanos, N. M. Clarke *et al.*, Phys. Lett. B **633**, 691 (2006).
[6] A. Cunsolo, A. Foti, G. Imme *et al.*, Nuovo Cimento **85**, 343 (1985).
[7] F. A. Souza, N. Carlin, C. Beck *et al.*, Eur. Phys. J. A **44**, 181 (2010).
[8] F. A. Souza, N. Carlin, C. Beck *et al.*, Nucl. Phys. A **834**, 420c (2010).
[9] D. Chattopadhyay, S. Santra, A. Pal *et al.*, Phys. Rev. C **94**, 061602(R) (2016).
[10] D. Scholz, H. Gemmeke, L. Lassen *et al.*, Nucl. Phys. A **288**, 351 (1977).
[11] H. Gemmeke, B. Deluigi, D. Scholz, and L. Lassen, Phys. Lett. B **96**, 47 (1980).
[12] D. Martinez Heimann, A. J. Pacheco, O. A. Capurro *et al.*, Phys. Rev. C **89**, 014615 (2014).
[13] R. Kanungo, T. Sinha, C. Samanta *et al.*, Nucl. Phys. A **599**, 579 (1996).
[14] C. M. Castaneda, H. A. Smith, Jr., P. P. Singh, and H. Karwowski, Phys. Rev. C **21**, 179 (1980).
[15] D. H. Luong, M. Dasgupta, D. J. Hinde *et al.*, Phys. Rev. C **88**, 034609 (2013).
[16] R. Ost, K. Bethge, H. Gemmeke *et al.*, Z. Phys. **266**, 369 (1974).

[17] C. Signorini, A. Edifizi, M. Mazzocco *et al.*, Phys. Rev. C **67**, 044607 (2003).
[18] N. Heide, D. K. Srivastava, and H. Rebel, Phys. Rev. Lett. **63**, 601 (1989).
[19] N. Heide, H. Rebel, V. Corcalciuc *et al.*, Nucl. Phys. A **504**, 374 (1989).
[20] S. Santra, V. V. Parkar, K. Ramachandran *et al.*, Phys. Lett. B **677**, 139 (2009).
[21] Y. Sakuragi, M. Yahiro, and M. Kamimura, Prog. Theor. Phys. Suppl. **89**, 136 (1986).
[22] J. P. Fernandez-Garcia, M. Zadro, A. Di Pietro *et al.*, Phys. Rev. C **92**, 054602 (2015).
[23] A. Gomez Camacho, A. Diaz-Torres, P. R. S. Gomes, and J. Lubian, Phys. Rev. C **93**, 024604 (2016).
[24] V. Valcovic, C. Joseph, S. T. Emerson, and G. C. Philips, Nucl. Phys. A **106**, 138 (1967).
[25] F. Cappuzzello, C. Agodi, D. Carbone, and M. Cavallaro, Eur. Phys. J. A **52**, 167 (2016).
[26] F. Cappuzzello, D. Carbone, M. Cavallaro, and A. Cunsolo, in *Magnets: Types, Uses and Safety*, edited by T. Akitsu (Tokyo University of Science, Tokyo, 2011), p. 1–63.
[27] A. Cunsolo, F. Cappuzzello, M. Cavallaro *et al.*, Eur. Phys. J.: Spec. Top. **150**, 343 (2007).
[28] M. Cavallaro, F. Cappuzzello, D. Carbone *et al.*, Eur. Phys. J. A **48**, 59 (2012).
[29] D. Carbone, F. Cappuzzello, and M. Cavallaro, Eur. Phys. J. A **48**, 60 (2012).
[30] F. Cappuzzello, M. Cavallaro, A. Cunsolo *et al.*, Nucl. Instrum. Methods Phys. Res., Sec. A **621**, 419 (2010).
[31] F. Cappuzzello, D. Carbone, and M. Cavallaro, Nucl. Instrum. Methods Phys. Res., Sec. A **638**, 74 (2011).
[32] M. Cavallaro, F. Cappuzzello, D. Carbone *et al.*, Nucl. Instrum. Methods Phys. Res., Sec. A **648**, 46 (2011).
[33] M. Cavallaro, F. Cappuzzelo, D. Carbone *et al.*, Nucl. Instrum. Methods Phys. Res., Sec. A **637**, 77 (2011).
[34] O. Sgouros, V. Soukeras, and A. Pakou (unpublished).
[35] A. Pakou, O. Sgouros, V. Soukeras *et al.*, Phys. Rev. C **95**, 044615 (2017).
[36] K. Rusek, K. W. Kemper, and R. Wolski, Phys. Rev. C **64**, 044602 (2001).
[37] K. Rusek, P. V. Green, P. L. Kerr, and K. W. Kemper, Phys. Rev. C **56**, 1895 (1997).
[38] R. Sherr, J. M. Blair, H. R. Kratz *et al.*, Phys. Rev. **72**, 662 (1947).
[39] F. Lahlou, R. J. Slobodrian, P. Bricault *et al.*, J. Phys. (France) **41**, 485 (1980).
[40] D. C. Kocher and T. B. Clegg, Nucl. Phys. A **132**, 455 (1969).
[41] A. S. Wilson, M. C. Taylor, J. C. Legg, and G. C. Phillips, Nucl. Phys. A **130**, 624 (1969).
[42] K. Sagara, H. Oguri, S. Shimizu *et al.*, Phys. Rev. C **50**, 576 (1994).
[43] G. Freier, E. Lampi, W. Sieator, and J. H. Williams, Phys. Rev. **75**, 1345 (1949).
[44] P. D. Miller and G. C. Phillips, Phys. Rev. **112**, 2043 (1958).
[45] I. J. Thompson, Comput. Phys. Rep. **7**, 167 (1988).